The EMBO Journal (2006) 25, 2189–2198 | © 2006 European Molecular Biology Organization | All Rights Reserved 0261-4189/06
www.embojournal.org

THE EMBO JOURNAL

Repair deficient mice reveal mABH2 as the primary oxidative demethylase for repairing 1meA and 3meC lesions in DNA

Jeanette Ringvoll[1], Line M Nordstrand[1], Cathrine B Vågbø[2], Vivi Talstad[2], Karen Reite[1], Per Arne Aas[2], Knut H Lauritzen[1], Nina Beate Liabakk[2], Alexandra Bjørk[1], Richard William Doughty[3], Pål Ø Falnes[1,4], Hans E Krokan[2] and Arne Klungland[1,5,*]

[1]Centre for Molecular Biology and Neuroscience and Institute of Medical Microbiology, Rikshospitalet-Radiumhospitalet HF, University of Oslo, Oslo, Norway, [2]Department of Cancer Research and Molecular Medicine, Norwegian University of Science and Technology, Trondheim, [3]Department of Safety, PCS Biology, GE Healthcare Bio-sciences, Oslo, Norway, [4]Department of Molecular Biosciences, University of Oslo, Oslo, Norway and [5]Department of Nutrition, Institute of Basic Medical Science, University of Oslo, Oslo, Norway

Two human homologs of the *Escherichia coli* AlkB protein, denoted hABH2 and hABH3, were recently shown to directly reverse 1-methyladenine (1meA) and 3-methylcytosine (3meC) damages in DNA. We demonstrate that mice lacking functional *mABH2* or *mABH3* genes, or both, are viable and without overt phenotypes. Neither were histopathological changes observed in the gene-targeted mice. However, in the absence of any exogenous exposure to methylating agents, mice lacking mABH2, but not mABH3 defective mice, accumulate significant levels of 1meA in the genome, suggesting the presence of a biologically relevant endogenous source of methylating agent. Furthermore, embryonal fibroblasts from mABH2-deficient mice are unable to remove methyl methane sulfate (MMS)-induced 1meA from genomic DNA and display increased cytotoxicity after MMS exposure. In agreement with these results, we found that *in vitro* repair of 1meA and 3meC in double-stranded DNA by nuclear extracts depended primarily, if not solely, on mABH2. Our data suggest that mABH2 and mABH3 have different roles in the defense against alkylating agents.

The EMBO Journal (2006) **25,** 2189–2198. doi:10.1038/sj.emboj.7601109; Published online 27 April 2006
Subject Categories: genome stability & dynamics
Keywords: AlkB; DNA repair; knockout; mouse; oxidative demethylation

Introduction

Alkylated bases in DNA are repaired by three principally different mechanisms, depending on the type of lesion. These include (1) DNA glycosylases, which initiate base excision repair at methylated bases by removing the methylated base (Laval, 1977; Chen *et al*, 1989); (2) suicidal methyltransferases, which transfer the methyl group from the DNA onto a cysteine residue in the transferase itself (Tano *et al*, 1990) and (3) the newly identified AlkB family of dioxygenases, which directly reverse DNA base damage by oxidative demethylation (Duncan *et al*, 2002; Falnes *et al*, 2002; Trewick *et al*, 2002; Aas *et al*, 2003). The importance of efficient alkylation repair is further emphasized by the existence, within the same organism, of more than one enzyme representing each of these repair strategies. An example is the well-known AlkA and Tag DNA glycosylases, which initiate base excision repair at alkylated bases in *Escherichia coli* (*E. coli*) (Clarke *et al*, 1984). Tag is constitutively expressed, whereas AlkA is induced as part of the adaptive response (Karran *et al*, 1979; Evensen and Seeberg, 1982; Karran *et al*, 1982). All three strategies for alkylation repair are conserved from *E. coli* to man (Sedgwick, 2004).

The conservation of enzymes specialized to repair methylated bases in DNA implies that naturally occurring methylating agents are widespread (Sedgwick, 2004). Such methylation can occur endogenously by the methyl donor *S*-adenosyl-methionine (SAM) (Barrows and Magee, 1982; Rydberg and Lindahl, 1982; Naslund *et al*, 1983) or by exposure to exogenous alkylating agents, originating from food, cigarette smoke, occupational chemicals or chemotherapeutics (Sedgwick, 2004). Methylating agents can react with DNA at several different sites on the DNA bases, including all the exocyclic oxygens and most ring nitrogens (Lindahl, 1993). The degree of alkylation at a given site depends not only on the mode of the chemical reaction (S_N1 or S_N2) but also on whether the DNA is in a single-stranded (ssDNA) or double-stranded (dsDNA) state (see below). AlkB has been thought to be involved in the cellular defense against methylation damage ever since it was discovered that *alkB* mutant *E. coli* cells were hypersensitive towards methylating agents (Kataoka *et al*, 1983; Kataoka and Sekiguchi, 1985), but it took almost 20 years to reveal the function of AlkB. A major breakthrough came when Sedgwick and co-workers demonstrated that AlkB repaired lesions that were specifically introduced in ssDNA, but not in dsDNA, and suggested that 1meA and 3meC were substrates for AlkB (Dinglay *et al*, 2000). Soon after, a landmark bioinformatics study placed the AlkB family of proteins in the superfamily of 2-oxoglutarate and Fe(II)-dependent oxygenases (Aravind and Koonin, 2001). By combining these clues, two independent studies showed that AlkB from *E. coli* was indeed a 2-oxoglutarate- and Fe(II)-dependent DNA repair enzyme capable of repairing 1meA and 3meC by oxidative demethylation (Falnes *et al*, 2002; Trewick *et al*, 2002). The substrate specificities of bacterial and human AlkB proteins have recently been extended to include 1-methylguanine (1meG) and

*Corresponding author. Centre for Molecular Biology and Neuroscience and Institute of Medical Microbiology, Rikshospitalet-Radiumhospitalet HF, University of Oslo, 0027 Oslo, Norway. Tel.: +47 23074072; Fax: +47 23074061; E-mail: aklungla@medisin.uio.no

Received: 17 October 2005; accepted: 31 March 2006; published online: 27 April 2006

3-methylthymine (3meT), as well as ethylated bases (Delaney and Essigmann, 2004; Falnes, 2004; Koivisto *et al*, 2004). Thus, substrates for AlkB comprise all the lesions resulting from methylation at the N1 position of purines and N3 position of pyrimidines. These positions are structurally equivalent (the numbering of purine and pyrimidine bases is different) and shielded from methylation in the context of dsDNA, as they are involved in hydrogen bonding in Watson–Crick base pairing. Recently, the substrates of AlkB was expanded to include 1,*N*(6)-ethenoadenine and 3,*N*(4)-ethenocytosine (Delaney *et al*, 2005).

Bioinformatics indicate the existence of eight different dioxygenases of the AlkB family in mammalian cells, denoted ABH1–ABH8 (AlkB Homolog) (Kurowski *et al*, 2003). However, only two of the corresponding human proteins, hABH2 and hABH3, have been shown to possess a similar repair activity as AlkB from *E. coli* (Duncan *et al*, 2002; Aas *et al*, 2003). Besides removing lesions from DNA, AlkB and hABH3 also repair 1meA and 3meC in RNA (Aas *et al*, 2003). Purified AlkB and hABH3 were recently found to restore the biological function of mRNA and tRNA inactivated by chemical methylation (Ougland *et al*, 2004). Furthermore, chemically methylated *E. coli* tRNA was demethylated in an AlkB-overexpression strain, revealing a putative role for such repair enzymes *in vivo* (Ougland *et al*, 2004). In contrast, purified hABH2 displayed undetectable or very low levels of activity against methylated RNA species (Aas *et al*, 2003; Ougland *et al*, 2004). Whereas ds nucleic acids are the favored substrates for hABH2, ss substrates are preferred by hABH3 (Falnes *et al*, 2004; Koivisto *et al*, 2004), and these proteins also display distinct subnuclear localization patterns (Aas *et al*, 2003).

An elegant study by Delaney and Essigmann (2004) investigated the relative mutagenicity, genotoxicity and repair of 1meA, 3-ethylcytosine (3eC), 1meG and 3meT in *E. coli*. All these lesions blocked replication in repair-deficient cells, whereas their miscoding properties varied significantly. Mutations observed included G to T and G to A base substitutions, which are also observed in organisms exposed to alkylating agents (Delaney and Essigmann, 2004). It was concluded that AlkB suppresses both genotoxicity and mutagenicity at physiologically realistic levels of alkylated lesions.

In order to investigate the relevance of DNA repair by ABH2 and ABH3 *in vivo*, we have generated gene-targeted mice lacking functional genes coding for these two proteins. Novel assays have been developed to measure the presence of methyl lesions in mouse genomic DNA, as well as to characterize the repair proficiency of extracts and cells prepared from mouse tissues.

Results

Generation of mABH2 and mABH3 null mice

The two murine AlkB homologs, mAHB2 and mABH3, are relatively small basic proteins spanning 239 and 286 amino acids, respectively. The identity between mABH2 and hABH2 is 75.1% and the identity between mABH3 and hABH3 is 85.7%, suggesting similar activities (Lee *et al*, 2005). Sequence alignment shows that the three residues (His 149/191, Asp 151/193 and His 214/257), presumed to constitute the Fe(II)-binding cluster in *E. coli* AlkB, are conserved in the mouse proteins. The importance of some of these residues was recently verified by site-directed mutagenesis of mouse and human ABH2 and ABH3 (Lee *et al*, 2005). Based on comparison with other 2-oxoglutarate and Fe(II)-dependent oxygenases, a conserved arginine (Arg 226 in mABH2 and Arg 269 in mABH3) most likely binds the 5-carboxylate of the 2-oxoglutarate co-substrate (Mukherji *et al*, 2001; Aas *et al*, 2003; Valegard *et al*, 2004). The Fe(II)-binding cluster and the conserved arginine are encoded by exon 4 of the *mABH2* gene and exons 8 and 10 of the *mABH3* gene. To eliminate activity of the enzymes, exon 4 of *mABH2* and exons 7 and 8 of *mABH3* were targeted, as outlined in Figures 1 and 2 and Supplementary Figure 1.

Mendelian inheritance of mutated alleles in single and doubleknockouts

Genotyping of more than 40 live-born mice produced by inter-mating of F_1 heterozygotes (one litter for each genotype is presented in Supplementary Figure 1F) showed that *mABH2* and *mABH3* null mice are viable. Homozygous mutant mice were recovered in F_2 litters at frequencies consistent with Mendelian segregation (data not shown) and were phenotypically indistinguishable from their heterozygous and wild-type siblings. Furthermore, interbreeding of *mABH2* and *mABH3* null mice generated homozygous double mutants at the expected ratio in F_2. Null animals remained viable and apparently healthy into adulthood with no overt

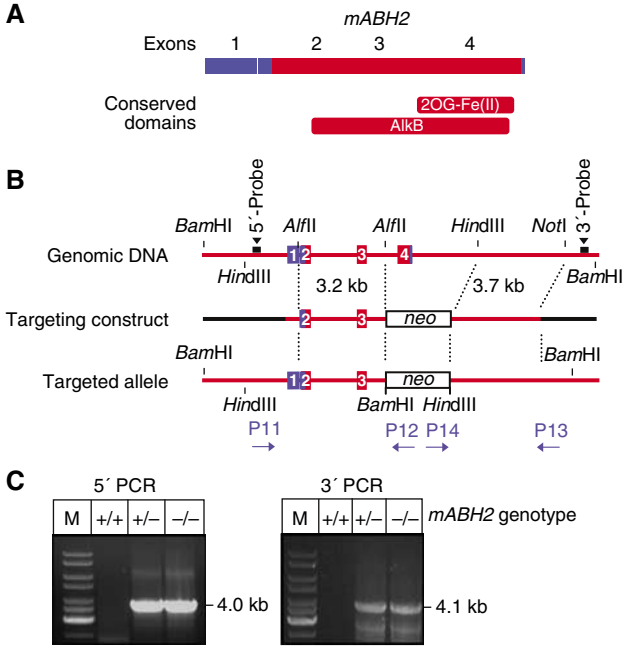

Figure 1 Targeted disruption of the murine *mABH2* locus. (**A**) Overview of the *mABH2* exons with the location of the 2-oxoglutarate- and Fe(II)-dependent oxygenase domain as well as the AlkB domain. Translated regions are shown in red, whereas untranslated regions are in blue. (**B**) Physical map of the genomic DNA containing the *mABH2* gene with the location of exons 1, 2, 3 and 4. Genomic fragments were subcloned on both sides of the *neo* gene to generate a construct with a deleted 3.2 kb fragment, including exon 4. The positions of the 5′ and 3′ probes used to screen ES cells for correct targeting events are indicated, as are the restriction enzymes relevant for subcloning and genotyping by Southern hybridization. (**C**) Correct 5′ and 3′ targeting, left and right panel, of *mABH2* mice were analyzed by PCR. Details of ES-cell genotyping are outlined in Supplementary Figure 1.

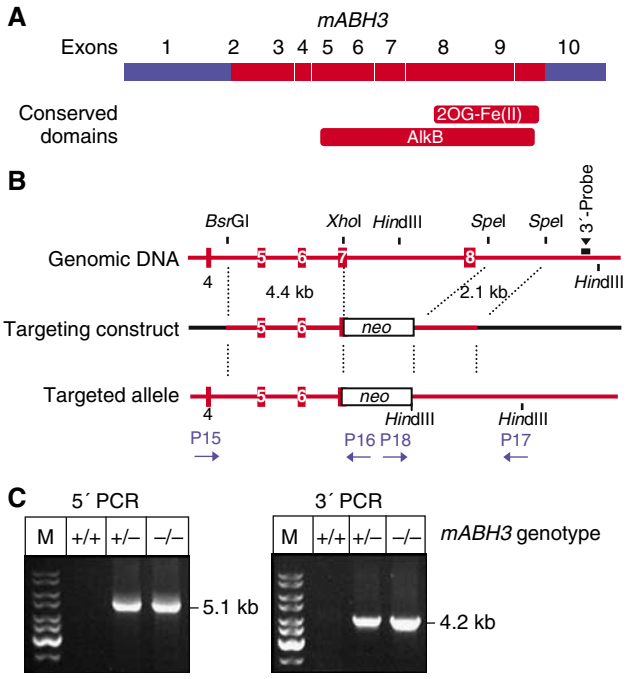

Figure 2 Targeted disruption of the murine *mABH3* locus. (**A**) Overview of the *mABH3* exons, as for *mABH2* above. (**B**) Physical map of the genomic DNA containing parts of the *mABH3* gene with the location of exons 4, 5, 6, 7 and 8. Genomic fragments were subcloned on both sides of the *neo* gene to generate a construct with a deleted 5.6 kb fragment including exon 8 and part of exon 7. The position of the 3′ probe is shown on the illustration for the genomic DNA, whereas the positions of the primers (Supplementary Table 1) used for PCR screening of ES-cells are indicated on the targeted allele. Restriction enzymes relevant for subcloning and genotyping by Southern analysis are indicated. (**C**) Correct 5′ and 3′ targeting, left and right panel, of *mABH3* mice were analyzed by PCR. Details of ES-cell genotyping are outlined in Supplementary Figure 1. Other details as in Figure 1.

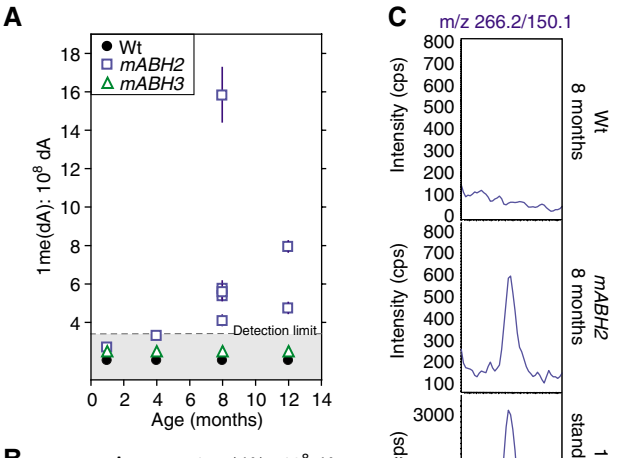

B

Individual	Age (months)	1me(dA) : 10^8 dA Sample a	Sample b
1	8	5.5	5.2
2	8	4.1	4.0
3	8	6.0	5.5
4	8	5.3	5.8
5	8	14.8	16.8
6	12	7.7	8.1
7	12	4.5	4.9

Figure 3 Accumulation of 1meA in aging repair-deficient mice. (**A**) Scatter diagram showing the accumulation of 1meA in genomic DNA from liver of 1-, 4-, 8- and 12-month-old wild-type, *mABH2*- and *mABH3*-targeted mice. Only 8- and 12-month-old *mABH2*-targeted mice had 1me(dA)-levels above the detection limit, which was approximately 3.5 1me(dA):10^8dA. Duplicates of 100 µg genomic DNA from two to four mice of each genotype were used at each time point. The steady-state level of 1meA was determined by the HPLC-MS/MS scheme described in the Materials and methods. (**B**) Numerical values of 1meA in genomic DNA from liver of 8- and 12–month-old *mABH2*-targeted mice plotted in panel A, with parallel determinations denoted as a and b. (**C**) HPLC-MS/MS chromatogram of 1me(dA) in genomic DNA from liver of 8-month-old wild-type (upper panel) and *mABH2*-targeted mice (middle panel), compared with 1me(dA) standard (lower panel).

phenotype. Although some *mABH2* and *mABH3* null mice have died before the age of 18 months, no obvious phenotype was observed (results not shown). The aging colonies of mice are now about 18-month old, except for the double knockouts at 12 months of age. Histopathological examination of four 18-month-old mice, each of wild-type, *mABH2* and *mABH3*, and two 12-month-old double knockouts, revealed no lesions or abnormalities that were considered to be related to genotype (Materials and methods). All lesions recorded were considered to be incidental.

Accumulation of 1meA in repair-deficient mice

To study the role of mABH2 and mABH3 for repair of erroneous endogenous methylation in DNA, genomic DNA was extracted from the livers of untreated wild-type, *mABH2* and *mABH3* knockout mice at different ages (Figure 3). The steady-state level of 1meA was determined at 1, 4, 8 and 12 months of age by the HPLC-MS/MS scheme, described in detail in Materials and methods. Two DNA samples, typically 100 µg, were purified from each liver, and 2–4 mice of each genotype were sacrificed at each time point. The 1meA levels were below the detection limit in untreated 1-month-old mice, regardless of the genotype. Likewise, no 1meA could be detected in wild-type and *mABH3* knockout mice at later time points. In contrast, 1meA accumulation was observed in 4-month-old *mABH2* null mice, although only slightly above the detection limit, with a further increase at 8 months (Figure 3A and B). We estimated that at 8 months of age, wild-type and *mABH3* knockout mice had accumulated less than 120 1meA per genome, whereas the corresponding number for the *mABH2* knockout was within the range 150–500. Significant accumulation of 1meA was also observed in two 12-month-old *mABH2* knockout mice. These results suggest that a substantial degree of aberrant methylation, producing 1meA lesions in DNA, occurs under normal physiological conditions.

Kinetics of 1meA repair in vivo

To assess the role of 1meA repair in living cells, mouse embryo fibroblast (MEF) cell lines established from the different mouse models were treated with the DNA methylating agent methyl methane sulfonate (MMS). Before examining the repair capacities in targeted cell lines, the repair kinetics of 1meA lesions induced by three different MMS concentrations (0.1, 0.5 and 2 mM) in wild-type cells were established (Figure 4A), and a substantial degree of repair was observed upon exposure to all three concentrations. The highest concentration of MMS (2 mM) was subsequently used in all the studies owing to more robust and accurate lesion detection. Repair was allowed to continue for up to 36 h after

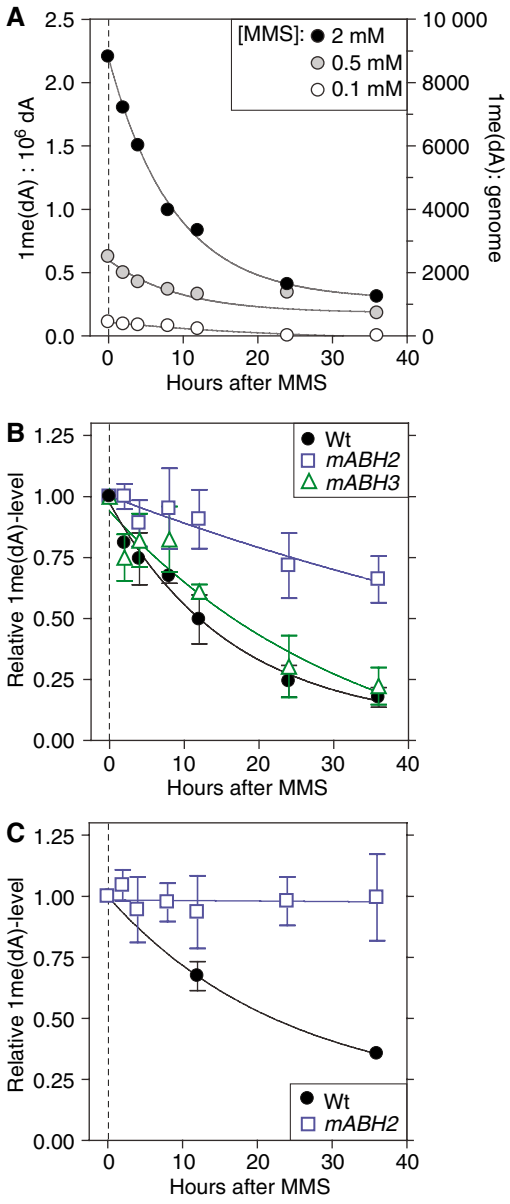

Figure 4 Kinetics of 1meA repair *in vivo*. (**A**) Kinetics of 1meA repair in wild-type MEF cells treated with 0.1, 0.5 and 2 mM of MMS. Cells were incubated with MMS for 1 h at 37°C, washed extensively and then allowed to repair DNA damages for up to 36 h before DNA isolation and HPLC-MS/MS identification of 1meA. One point represents approximately 10^6 cells and 50 μg of genomic DNA. (**B**) Kinetics of 1meA removal in wild-type, *mABH2*- and *mABH3*-targeted cells treated with 2 mM MMS. Further details are the same as for panel A. (**C**) Repair kinetics in replication arrested wild-type and mABH2-depleted cells incubated with 6 μM aphidicolin. Cells were treated with 2 mM of MMS for 1 h at 37°C, and then incubated with 6 μM aphidicolin for up to 36 h to investigate the DNA repair process under replication arrest. DNA isolation and HPLC-MS/MS identification of 1meA were carried out as described for panel B above.

removal of MMS. Genomic DNA was purified, and the amount of 1meA determined using HPLC-MS/MS (Figure 4). Extensive washing of the cells was essential to ensure that no residual MMS remained as this caused a substantial further increase of DNA methylation (results not shown). In wild-type cells exposed to 2 mM MMS for 1 h, the amount of 1meA present was reduced by more than 50% after 8 h; approximately 10% of the induced 1meA remained in the cells after 36 h (Figure 4A and B). Such repair kinetics are comparable to those observed for other base lesions (Klungland *et al*, 1999).

The repair kinetics of 1meA in *mABH3*-targeted cells was indistinguishable from those of wild-type cells (Figure 4B). In contrast, and in agreement with the data obtained regarding repair of 1meA and 3meC in cellular extracts presented below, only a small fraction of 1meA was repaired in *mABH2*-targeted cells. An approximate 10% reduction in the 1meA levels was observed after 8 h, whereas a reduction of 30% was observed after 36 h. All experiments were carried out in MEF cells grown to about 80% confluence. In order to eliminate dilution of the lesions due to DNA replication, the experiments were repeated in the *mABH2*-targeted cells with the addition of aphidicolin, which inhibits elongation of the replicons (Saintigny *et al*, 2001). The repair rate of 1meA in *mABH2*-targeted cells was further reduced with this treatment, and only a negligible fraction of 1meA was removed following 36 h incubation (Figure 4C). In order to exclude the possibility that aphidicolin inhibits 1meA repair, similar experiments were carried out in wild-type cells. No significant reduction in the repair rates was observed (Figure 4C).

Cellular sensitivity to methylating agent

E. coli mutants deficient in 3-methyladenine DNA glycosylase activity (*alkA* and *alkA tag*) are extremely sensitive to exposure of alkylating agents (Clarke *et al*, 1984), whereas the alkB mutant displays moderate sensitivity (Kataoka *et al*, 1983). MEFs and ES clones lacking the murine 3-methyladenine DNA glycosylase (Aag) are hypersensitive towards methylating agents (Engelward *et al*, 1996; Engelward *et al*, 1997), but much less so than in the *E. coli alkA tag* mutant. Based on these observations, a modest but significant sensitizing of *mABH2* cells and wild-type resistance of *mABH3* cells was expected (Figure 5). Wild-type growth rates are observed in all cell lines.

DNA substrates for 1meA and 3meC repair

Purified *E. coli* AlkB and the human homologs hABH2 and hABH3 are able to repair 1meA and 3meC in DNA by oxidative demethylation (Duncan *et al*, 2002; Falnes *et al*, 2002; Trewick *et al*, 2002; Aas *et al*, 2003). Taking advantage of the inability of the *Dpn*II restriction endonuclease to recognize a methylated GATC sequence, we established an *in vitro* assay for the repair of 1meA and 3meC by cellular extracts (Figure 6A and Supplementary Table 1). Repair of these lesions was monitored using a ds oligonucleotide containing either 1meA or 3meC within the GATC recognition sequence, and *Dpn*II cleavage would only occur if the lesion had been repaired by direct reversal. Initially, the *Bam*HI site was used to distinguish between methylated and unmethylated GGATCC. However, some *Bam*HI activity was observed on methylated sequences (results not shown). As illustrated in Figure 6B, 49-mer 5′-[^{32}P]end-labeled oligonucleotides containing 1meA or 3meC were cleaved to 22 nucleotide (nt)-labeled fragments only when the *Dpn*II digestion was preceded by incubation with AlkB, hABH2 or hABH3. A similar approach, utilizing methylation-sensitive restriction endonucleases, has previously been used successfully for the characterization of O6-alkylguanine-DNA alkyltransferase activity (Wu *et al*, 1987).

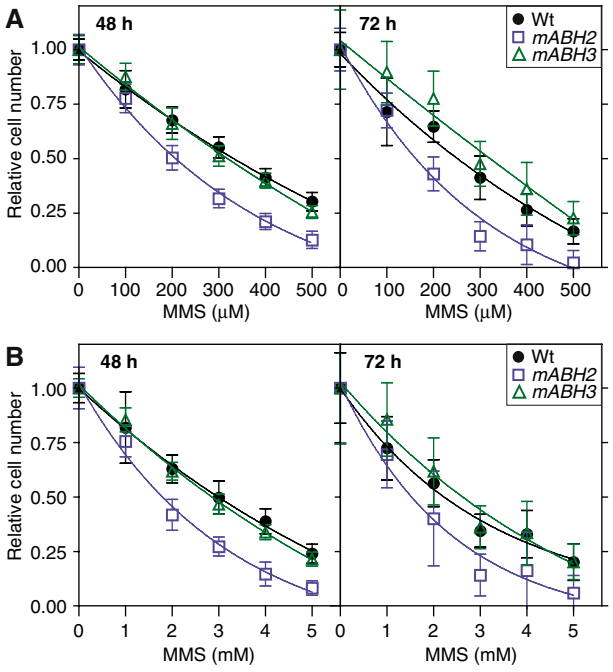

Figure 5 Effect of MMS on growth of MEF cell lines. Cells were seeded at a density of 2000 cells per well in 96-well plates ($n = 16$ for each measurement). Wild-type cell lines (Wt), *mABH2* or *mABH3* cell lines were used, as indicated. After 24 h culturing, the cells were treated with MMS continuously (**A**) or for 1 h (**B**). The results were expressed as cell numbers in MMS-treated cultures compared to untreated controls. (A) Cells treated for 48 or 72 h in media containing 0–500 μM MMS. (B) Cells were treated for 1 h with media containing 0–5 mM MMS, then washed with PBS before 200 μl fresh medium was added. Cell numbers were measured using the MTT-assay. Untreated MEF cell lines of the three genotypes had essentially similar growth rates.

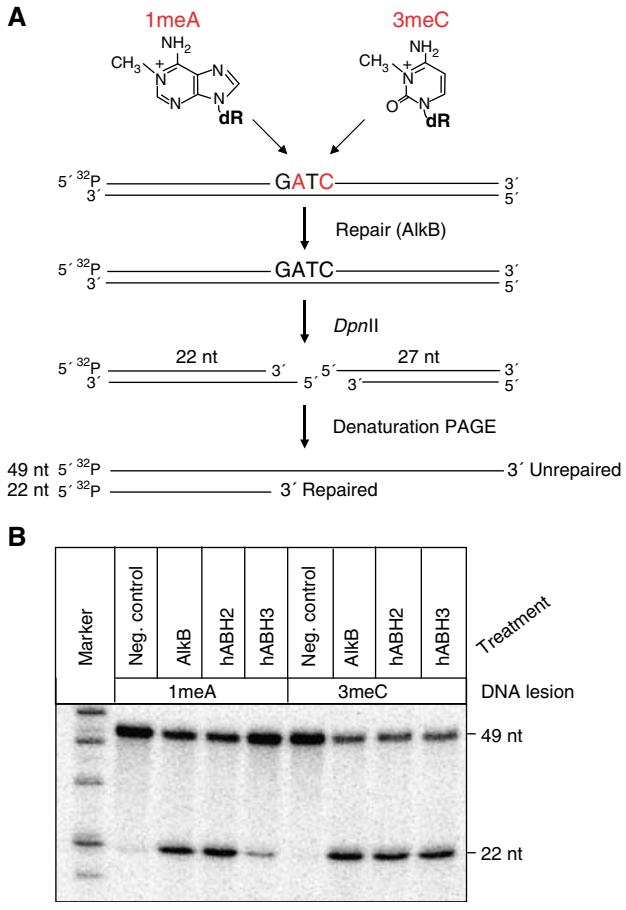

Figure 6 DNA substrates for 1meA and 3meC repair and activity of AlkB, hABH2 and hABH3. (**A**) The 1meA substrate consists of a 49 bp oligonucleotide with a methylated adenine in position 24, radioactively labeled at the 5′-end and hybridized to a complementary strand. The 3meC substrate has a methylated cytosine in position 26. The methylated base is located in the recognition site of the restriction enzyme *Dpn*II. To visualize the repair, we used the enzyme *Dpn*II, which is methylation sensitive and only cleaves the substrate if the methyl group is removed. An unrepaired substrate will result in a band of 49 nt, whereas the repaired and cleaved substrate will appear as a 22 nt band following denaturing PAGE. (**B**) Activity of purified AlkB, hABH2 and hABH3 on 1meA and 3meC in a dsDNA oligonucleotide. DNA substrates were incubated with purified enzymes as indicated, digested with *Dpn*II and separated by 20% denaturing PAGE. Labeled DNA was visualized by phosphorimaging. Both substrates were incubated with *Dpn*II, without previous repair, as a negative control.

Activity of hABH2 on dsDNA has been reported to be stimulated by magnesium, and maximal repair activity for hABH2 was obtained in the presence of 10 mM $MgCl_2$ (Falnes *et al*, 2004). In contrast, AlkB and hABH3 were not affected by magnesium. Consequently, we added magnesium to the reaction buffer in the case of mABH2, but not for AlkB or mABH3. Figure 6B demonstrates that hABH3 repairs 3meC more efficiently than 1meA. This is consistent with previous reports (Duncan *et al*, 2002; Aas *et al*, 2003; Lee *et al*, 2005). The repair of synthetic oligonucleotides by purified AlkB family enzymes was carried out to justify further use of these DNA substrates, and not to reveal the kinetics of the purified enzymes.

Enzyme activity in extracts from mABH2, mABH3 and mABH2/mABH3 null mice

Human ABH2 and ABH3 have previously been characterized *in vitro*. Purified hABH2 and hABH3 repair both 1meA and 3meC in DNA, although with a different preference for ds versus ss substrates (see Introduction). In order to assess the properties and relevance of these repair enzymes in cellular extracts, the duplex oligonucleotides described above were incubated with nuclear extracts from liver, testis and kidney, cleaved with *Dpn*II, and the reaction products analyzed by denaturing PAGE. $MgCl_2$ (10 mM) was added for optimal activity of mABH2. In addition, the amount of extract, DNA substrate and buffer conditions were titrated to obtain maximum repair activity and to minimize degradation of the DNA substrate (results not shown). The results indicate that mABH2 is the primary activity for repair of 1meA and 3meC in dsDNA in nuclear extracts (Figure 7 and Supplementary Figure 3). The repair activities at 1meA and 3meC lesions by mABH3-depleted cellular extracts are indistinguishable from the wild-type. Furthermore, extracts lacking both mABH2 and mABH3 have repair activities matching those of mABH2-depleted extracts. Similar results were observed with extracts from both liver and testis (Figure 7A and B and Supplementary Figure 3A).

To further investigate the repair of 1meA and 3meC lesions in extracts derived from gene-targeted mice, the amount of extract was varied between 0.5 and 10.0 μg and repair activities were quantified (Figure 7B). These data support the hypothesis that mABH2 is the primary, or only, demethylase for repairing 1meA and 3meC in dsDNA. Furthermore, very

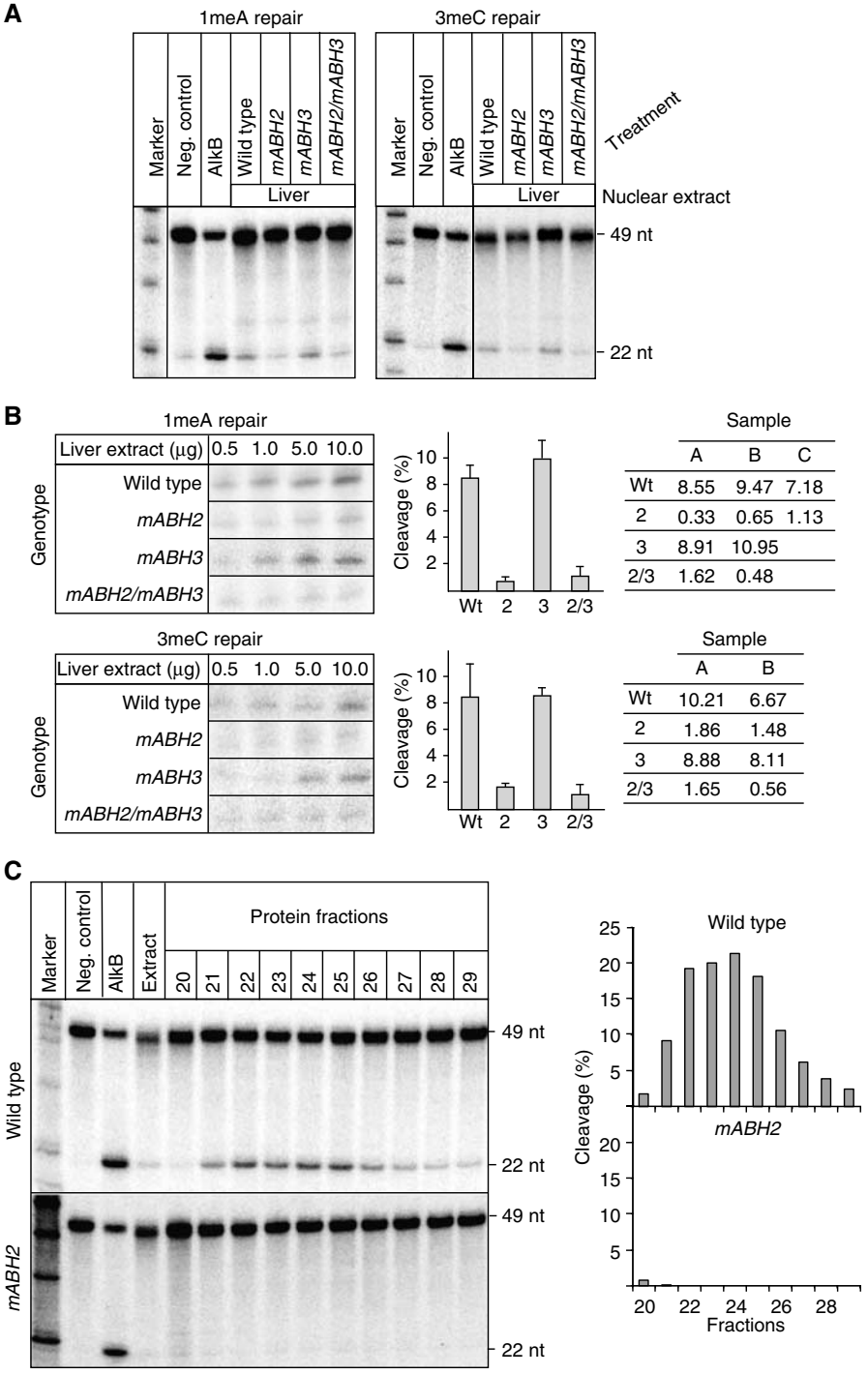

Figure 7 Repair of 1meA and 3meC in repair-deficient cellular extracts. Repair of 1meA and 3meC is demonstrated with the use of methylation-sensitive *Dpn*II cleavage, as above. (**A**) Repair of 1meA and 3meC. This panel shows the repair efficiency in nuclear extracts (5.0 μg) from the liver of wild-type, *mABH2*, *mABH3* and *mABH2/mABH3* null mice. No enzyme or protein extract was added in the negative control, whereas *E. coli* AlkB (100 ng) was used as a positive control. (**B**) Repair of 1meA and 3meC with increasing amounts of nuclear extracts. The two left panels show the 22 nt band for 1meA repair (top panel) and 3meC repair (bottom panel). Two to three assays were quantified for both substrates and the average of these, plus s.d., is shown in the bar graphs. The upper graph displays cleavage activity of 5.0 μg nuclear extract on the 1meA substrate, whereas the lower graph illustrates the activity of 10.0 μg extract on the 3meC substrate. Individual values of cleaved substrate are indicated. (**C**) Repair of 3meC in 0.75 μg freshly prepared protein fractions. Repair activities peak in fractions 22–25 and are dependent on mABH2 as no activity was observed in fractions from *mABH2* knockout mice. (**D**) Repair of 1meA and 3meC in peak fraction (fraction 24) show mABH2 dependence for 1meA and 3meC activity. The repair activity for both 1meA and 3meC is dependent on the amount of protein added (**E**) and the incubation time (**F**). In panel F, 0.75 μg was added to each reaction. The repair time was 30 min, if not indicated.

low, but detectable, repair activity was observed in nuclear wild-type extracts from kidney, a tissue with low expression of *mABH2* (Supplementary Figure 3C and results not shown).

We observed a low but reproducible and robust repair activity in extracts from mice having functional mABH2. To substantiate our findings somewhat, we attempted to

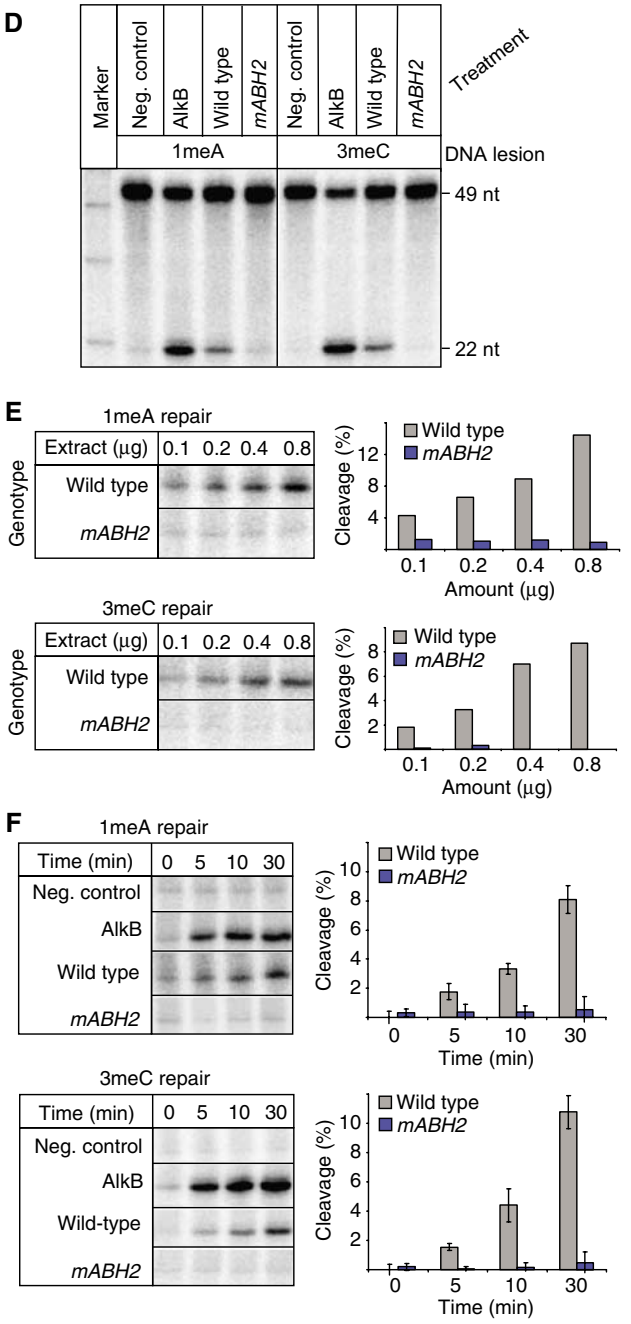

Figure 7 continued.

up-concentrate the repair activity, taking advantage of the observation that recombinant hABH2 elutes as a sharp peak from a cation exchange column at pH 8.0 and 370 mM NaCl. Indeed, when nuclear extracts prepared from the livers of 10 wild-type mice were subjected to cation exchange chromatography, the repair activity eluted at the expected NaCl concentration, and the repair efficiency obtained with the peak fractions were several fold higher than in the case of the unfractionated extracts. Significant repair was obtained with as little as 0.2 μg protein from peak fractions (Figure 7C–F). Again, the repair activity clearly appears to represent mABH2, as no activity was observed neither in the eluted fractions nor in the flow-through, when livers from *mABH2* mice were used (Figure 7C and results not shown). The activity was dependent on the amount of protein added and incubation time (Figure 7E and F). This purification scheme was also followed with nuclear extracts prepared from kidney, a tissue with low expression of *mABH2*. As expected, the repair activity was significantly reduced compared to the liver (Supplementary Figure 3C). However, detectable activity could be obtained from fractionated wild-type nuclear extracts from kidney. Again, no activity was detected in mABH2-deficient extract. ss linear DNA is rapidly degraded in cellular extracts. In order to further elucidate the role of mABH3, we are currently attempting to establish repair assays by using exonuclease protected circular ssDNA containing 1meA and 3meC.

Discussion

Endogenous DNA methylation

Harmful, nonenzymatic, and possible enzymatic, DNA methylation and its repair is a topic that recently has attracted a great deal of interest, owing to the discovery of a novel, evolutionary conserved mechanism for repairing methylation damage. Both mammalian and bacterial AlkB proteins were shown to repair certain methylated bases *in vitro*, as well as to correct the repair deficiency of *alkB* mutant *E. coli* (Duncan *et al*, 2002; Aas *et al*, 2003). We demonstrate that *mABH2*, but not *mABH3*, null cells display a defect in removing methyl lesions from DNA and that spontaneously arising methyl lesions accumulate in the genome of the *mABH2*-targeted mice. This represents the first demonstration of accumulated, spontaneous methylation damage in repair-deficient cells, further substantiating the notion that repair of endogenously generated lesions is an important role for methylation repair. In accordance with this, the AlkB mechanism is well conserved between organisms that would be expected to experience very different loads of methylation from exogenous sources (Falnes and Rognes, 2003).

Nonenzymatic methylation of DNA is known to arise endogenously in bacteria, and DNA alkylation repair limits spontaneous mutations (Mackay *et al*, 1994; Taverna and Sedgwick, 1996). In mammalian cells, several possible sources of nonenzymatic methylation by methyl group donors exist, but only the universal methyl donor SAM has been investigated to any extent. More than 20 years ago, several studies addressed the relevance of endogenous DNA methylation by SAM (Barrows and Magee, 1982; Rydberg and Lindahl, 1982; Naslund *et al*, 1983) and concluded that SAM does methylate DNA nonenzymatically. Based on experiments with highly purified [^{3}H methyl]SAM, Rydberg and Lindahl (1982) estimated that intracellular SAM could result in DNA methylation at a level similar to that expected to occur as a result of the continuous exposure of cells to 20 nM MMS (Rydberg and Lindahl, 1982).

In our MMS-exposure experiments, we measured the formation of approximately one 1meA lesion per 10^6 adenines per millimolar MMS per hour, whereas spontaneous lesions accumulated in *mABH2*-targeted mice at an approximate rate of one lesion per 10^7 adenines per year, that is at a rate roughly five orders of magnitude lower, and well comparable to that expected from exposure to nanomolar concentrations of MMS in the absence of repair (assuming a linear relationship between lesion formation and MMS dose; 1 mM/10^5 = 10 nM). Thus, the intracellular concentration of methy-

lating agents may well be close to the value estimated by Rydberg and Lindahl (1982).

The biological roles of mABH2 and mABH3

The mammalian AlkB homologs ABH2 and ABH3 both have the ability to demethylate 1meA and 3meC lesions in DNA, but there are also some important differences between these enzymes. Whereas hABH2 displayed a moderate, magnesium-dependent preference for dsDNA, hABH3 favored ssDNA (Falnes *et al*, 2002; Aas *et al*, 2003; Koivisto *et al*, 2004), and similar results have recently been obtained in the case of mABH2 and mABH3 (Lee *et al*, 2005). Moreover, the subcellular localization of hABH2 and hABH3 was found to be very different (Aas *et al*, 2003). hABH2 was exclusively nuclear and showed a cell-cycle-dependent distribution; it was found in replication foci during the S-phase, and accumulated in the nucleoli of non-S-phase cells. hABH3, on the other hand, was found both in the cytosol and in the nucleus, but was excluded from nucleoli. Interestingly, hABH3, but not hABH2, was also shown to efficiently demethylate lesions in RNA. Actually, the data presented here might strengthen the possible role of mABH3 as a specialized RNA repair enzyme, and experiments along these lines are underway. Our data indicate that mABH3 (and probably also hABH3) does not play a major role in removing 1meA and 3meC lesions from genomic DNA. High-resolution structure of substrate and product complexes of AlkB was recently published (Yu *et al*, 2006). The sequence divergence in the nucleotide-recognition lids between AlkB, ABH2 and ABH3 may be related to their significantly different affinity for different nucleic acid substrates observed *in vitro* (Aas *et al*, 2003; Falnes *et al*, 2004), and thus support our *in vivo* observations. However, our assays might lack the sensitivity required to identify repair at ss regions of DNA occurring transiently *in vivo* within transcription bubbles and replication forks. Furthermore, it is possible that mABH3 might have other, favored, DNA substrates.

Mammalian AlkB homologs

ABH1, the mammalian AlkB homolog with the strongest sequence similarity to the *E. coli* AlkB protein, was also the first one to be identified (Wei *et al*, 1996). However, no DNA repair activity has been demonstrated in the case of this protein, despite numerous efforts. Combination of biochemical and bioinformatics approaches led to the discovery of DNA repair by dioxygenases in bacteria and humans, and today the AlkB family in mammals consists of eight members, denoted as ABH1–ABH8 (Kurowski *et al*, 2003). However, only in the case of ABH2 and ABH3 has an *in vitro* activity been reported (Lee *et al*, 2005). It is tempting to speculate that mABH1 may carry out repair *in vivo*, although no activity has been ascribed to the purified protein so far. In order to evaluate this further, *mABH2* knockout mice are currently being interbred with the *mABH1*-targeted mice (*mABH1*-targeted mice are viable—Nordstrand, Ringvoll and Klungland; unpublished data). The large number of lesions identified in DNA, as well as the comprehensive list of modified RNA nucleotides, suggest that the remaining ABH members may exhibit various exciting properties with regard to the repair and regulation of DNA and RNA species (Rozenski *et al*, 1999; Kurowski *et al*, 2003).

Materials and methods

Construction of targeting vectors for mABH2 and mABH3

A specific murine probe of the *mABH2* sequence was amplified from murine genomic DNA by polymerase chain reaction (PCR) (primers 1 and 2, Supplementary Table 1) and was used to screen a mouse 129/SvJ lambda genomic library (Stratagene). A genomic clone of ~12.0 kilobases (kb) spanning the whole coding region of the *mABH2* gene was used to produce the targeting construct. The correct recombination event will result in the deletion of ~3.2 kb of the *mABH2* gene, containing the exon 4 sequence, which includes the conserved 2-oxoglutarate and Fe(II)-dependent oxygenase domain as well as the AlkB domain (Figure 1A and B). The resulting construct, based on the vector pGT-N38 (New England Biolabs), possesses homologous arms of 3.7 and 3.2 kb, which flank the *neo* gene.

Primers 3 and 4 (Supplementary Table 1) were used to identify the *mABH3* gene. A genomic clone of ~13.8 kb spanning exons 5–8 of the *mABH3* gene was used to produce the targeting construct, together with the vector pGT-N28 (New England Biolabs). The correct recombination event will result in the deletion of ~5.6 kb of the *mABH3* gene (Figure 2A and B). The deleted area, including exon 8 and part of exon 7, contains sections of the conserved 2-oxoglutarate- and Fe(II)-dependent oxygenase domain as well as the AlkB domain (Figure 2A). The resulting construct possesses homologous arms of 4.4 and 2.1 kb, which flank the *neo* gene. The accuracy of the targeting construct was verified as above. Verification of correct ES-cell targeting is outlined in Supplementary Figure 1.

Histopathology

The following tissues were collected from wild-type, *mABH2*, *mABH3* and *mABH2/mABH3* mice and fixed in 10% neutral-buffered formalin: the skeletal muscle, ovary, uterus, vagina (females) or testis, epididymis, accessory sex glands (males), skin, mesenteric lymph node, liver, small and large intestines, pancreas, lungs, spleen, kidney, heart, thymus, urinary bladder, adrenal gland, sternum, cervical, thoracic and lumbar spinal cord, pituitary gland, brain and eye. After fixation, tissues were trimmed, embedded in paraffin, sectioned at 5 μm and stained with hematoxylin and eosin using standard methods previously described (Relyea *et al*, 2000; Brayton *et al*, 2001) All tissues were examined by a veterinary pathologist using light microscopy.

Preparation of genomic DNA from mouse liver

Approximately 100 μg of mouse liver was incubated with 50 mM Tris (pH 8.0), 100 mM EDTA, 0.5% SDS and 250 μg proteinase K at 55°C over night. After extraction of DNA with phenol/chloroform and addition of 0.1× volume of 3 M sodium acetate and 2× volumes of 100% ethanol, the DNA was spooled onto a fused-end Pasteur pipette. Finally, the DNA was rinsed in 70% ethanol and air dried for 15 min at room temperature and dissolved in 100 μl dH_2O. The DNA concentration was determined using NanoDrop 3.0.1 and processed further as described below.

HPLC-MS/MS analysis

DNA samples (typically 50 μg) or 1meA-containing oligonucleotide standards were enzymatically hydrolyzed to nucleosides by using nuclease P1, snake venom phosphodiesterase and alkaline phosphatase (Crain, 1990). This was followed by the addition of 3× volume of methanol and centrifugation at 16 000 *g* for 30 min. The supernatants were dried under vacuum, and the resulting residues dissolved in 50 μl 0.1% formic acid/5% methanol in water (v/v), for 1-methyldeoxyadenosine (1me(dA)) analysis by HPLC-MS/MS. A portion of each sample was diluted to 1:25 000 for quantitation of the corresponding deoxyadenosine (dA).

HPLC apparatus consisted of an HP1100 system (Agilent Technologies) with binary pump, autosampler and solvent degasser. Gradient chromatographic separation of 1me(dA) analytes was performed on a Zorbax SB-C18 2.1 × 150 mm^2 i.d. (3.5 μm) reverse phase column equipped with an Eclipse XDB-C8 2.1 × 12.5 mm^2 i.d. (5 μm) guard column (both from Agilent Technologies), at ambient temperature and a flow rate of 0.2 ml/min. The mobile phase consisted of A (0.1% formic acid in water) and B (0.1% formic acid in methanol), in a gradient elution starting with 95% A/5% B for 3.5 min, followed by a 7 min linear gradient of 5–50% B, and finally 25 min re-equilibration with the initial mobile phase conditions.

Chromatographic analysis of dA was performed under isocratic conditions on a Supelcosil LC-C18-S $4.6 \times 150\,mm^2$ i.d. (5 μm) reverse phase column (Sigma-Aldrich). This was maintained at ambient temperature, with a mobile phase of 80% A/20% B at a flow rate of 1 ml/min.

Online mass spectrometry detection was performed using an Applied Biosystems/MDS Sciex 4000 hybrid triple quadrupole/linear ion trap mass spectrometer (Applied Biosystems Sciex) with TurboIonSpray probe operating in positive electrospray ionization mode. The analytes were monitored in the multiple-reaction monitoring mode, using the mass transition 266.2→150.1 for 1me(dA) and 252.2→136.1 for dA.

Repair of 1meA in MEF lines and preparation of genomic DNA

MEF cells at 80% confluence were treated with the indicated doses of MMS for 1 h at 37°C. Following two rinses with PBS and replacement of the media, cells were incubated for up to 36 h under the cell culture conditions described. Cells were trypsinized, re-suspended in DMEM, pelleted at 4000 *g* for 5 min at 4°C, washed in PBS and collected at 4500 *g* for 3 min at 4°C. DNA was isolated as described in the Wizard®Genomic DNA Purification protocol (Promega) before HPLC-MS/MS identification of 1meA.

Furthermore, in *mABH2* null cells, repair of 1meA was studied under replication arrest. Following MMS treatment for 1 h at 37°C and rinsing twice with PBS, 6 μM aphidicolin (Calbiochem) was added to the fresh media. The cells were incubated for up to 36 h, and then harvested. DNA was isolated and finally separated using HPLC-MS/MS to identify 1meA as described above.

Cell culture and MMS exposure

Spontaneously immortalized clonal MEF cell lines were established from individual 13.5-day-old embryos (E13.5) obtained from heterozygous crossings (Hogan *et al*, 1994). All MEF lines were cultured at 37°C with 5% CO_2 in Dulbecco's modified Eagle's medium (DMEM) with high glucose, without L-glutamine (BioWhittaker™, BE12-614F), supplemented with 12.8% fetal bovine serum (PAA GmbH, A15-043), 0.3 mg/ml glutamine (BioWhittaker™, DE17-605E), 100 U/ml penicillin and 0.1 mg/ml streptomycin (BioWhittaker™, DE17-602E). The genotype of each cell line was determined by PCR as shown in Supplementary Figure 1F. The tetrazolium cytotoxicity assay (MTT) was performed basically as described (Espevik and Nissen-Meyer, 1986). The cells were seeded in 96-well plates with 2000 cells/well in 200 μl medium. Cells were exposed to medium containing MMS in culture medium either continuously (200 μl medium per well, 0–500 μM) or for 1 h (100 μl/well, 0–5 mM), 24 h after seeding. Cell numbers were measured using the MTT assay.

Protein purification

AlkB, hABH2 and hABH3 were purified as previously described (Aas *et al*, 2003).

Preparation of protein extracts

Organs were removed, quickly frozen on dry ice and stored at −80°C until use. Nuclear extracts were prepared as described previously (Klungland *et al*, 1999). A concentration of approximately 4 mg/ml should be expected. Fractionation of nuclear extracts was performed on a cation exchange Resource S 1 ml column (GE Healthcare) by FPLC ÄKTA (GE Healthcare). The nuclear extract prepared from 10 pooled livers/kidneys was centrifuged at 13 000 *g* for 5 min and loaded to the column at 0.5 ml/min. The proteins were eluted with an NaCl gradient (Buffer A: 50 mM NaCl/50 mM Tris pH 8.0/2 mM DTT; Buffer B: 2 M NaCl/50 mM Tris pH 8.0/2 mM DTT) increasing the NaCl concentration with 0–25% Buffer B from fraction 1 to 30 and collected in 0.5 ml fractions at 0.5 ml/min. Fractions 1–30 were tested for repair activity. The procedure was carried out at 4°C.

Preparation of oligonucleotide substrates

A 49-mer oligonucleotide containing either *N*-1-methyl-dA (1meA substrate, Supplementary, Table 1) or *N*-3-methyl-dC (3meC substrate, Supplementary Table 1) was provided by ChemGenes (ChemGenes Corporation). The natural deoxynucleoside phosphoramidites were employed using standard procedures. The methylated deoxy CED-OP used were 5′-DMT-N1-Methyl deoxy Adenosine (n-fmoc) CED OP (Catalog No.: ANP-6121) and 5′-DMT-N3-Methyl deoxy Cytidine (n-bz) CED OP (Catalog No.: ANP-3851). After oligonucleotide synthesis, deprotection was performed using 28% ammonium hydroxide at 55°C for 10 h. Oligonucleotides were purified from the deprotection solution by using a Puri-Pak purification cartridge and 5′-DMT-ON protected crude oligonucleotides. The oligonucleotides were eluted as DMT-ON oligonucleotides, and then treated with 80% acetic acid for 15 min at 37°C before being repurified on a Puri-Pak cartridge and lyophilized. A control oligonucleotide (Supplementary Table 1) was provided by Invitrogen. All oligonucleotides included phosphorothioate linkages at their 5′ and 3′ ends to reduce exonucleolytic attack.

The oligonucleotides were end-labeled at the 5′ terminus. The labeling reaction contained 28 pmol of the oligonucleotide, 1.48MBq/0.04 mCi [γ-^{32}P]ATP (Amersham), 20 U T4 polynucleotide kinase (New England Biolabs), TSE-buffer (20 mM Tris–HCl pH 9.5/1 mM spermidin HCl/0.1 mM EDTA) and appropriate kinase buffer in a total volume of 60 μl (incubation for 45 min at 37°C). Equal molar amounts of the complementary oligonucleotide (Supplementary Table 1) containing either a thymine (T) or a guanine (G) residue opposite to the *N*-1-methyl-dA or *N*-3-methyl-dC, respectively, were then added to form duplex DNA substrate. This was incubated for 2 min at 90°C and then allowed to cool slowly to room temperature. End-labeled oligonucleotide substrates were purified following separation on a nondenaturing 20% PAGE gel.

DNA repair reactions

In order to avoid exonucleolytic degradation of the oligonucleotide substrates during incubation with cellular extracts, the optimal amount of substrate and nuclear extract were determined by titration (results not shown). A 50 μl reaction mixture containing 50 mM Tris, pH 8.0, 2 mM ascorbic acid, 100 μM 2-oxoglutarate, 40 μM $FeSO_4$ and approximately 150 fmol ^{32}P-labeled ds oligonucleotide substrate (which roughly correspond to 16 000 c.p.m. for the freshly prepared 1meA substrate and 9000 c.p.m. for the freshly prepared 3meC substrate), containing either an *N*-1-methyl-dA or *N*-3-methyl-dC lesion located within a palindromic site for recognition by restriction endonucleases, was incubated at 37°C for 30 min with either 100 ng enzyme (AlkB, hABH2 or hABH3) or the amount of nuclear extracts indicated in the figures. In order to improve the repair, 10 mM $MgCl_2$ was added to reactions containing hABH2 and nuclear extracts. Reactions with purified enzymes were incubated at 50°C for 10 min to inactivate the enzymes. All other reactions were terminated by adding EDTA to 18 mM, SDS to 0.4% and proteinase K to 0.4 μg/μl, and incubating at 37°C for 30 min. The DNA was precipitated by adding 25 μg tRNA (Roche), NaAc pH 5.5–0.3 M and 3× volume of ice-cold 100% ethanol, and placed at −20°C overnight. The precipitated DNA was washed in 70% ethanol and dissolved in 25 μl dH_2O.

AlkB and its homologs oxidize the methyl group, resulting in direct reversal of the damage without cleaving the DNA strand. The restriction enzyme *Dpn*II is methyl sensitive and was used to distinguish methylated and repaired oligonucleotides. The site of the damage is within the *Dpn*II recognition sequence (5′-GATC-3′). An aliquot of 7 μl from reactions with purified enzymes or the precipitated DNA from reactions with nuclear extract was cleaved by 20U *Dpn*II (New England Biolabs) at 37°C for 1 h. Oligonucleotides were resolved by 20% denaturating PAGE gel. They were visualized and quantified using an ImageQuant (Typhoon 9410). Assays were repeated with organs from two (or three) different mice and gave consistent results.

Supplementary data

Supplementary data are available at *The EMBO Journal* Online.

Acknowledgements

We are grateful to Cecilie G Castellanos, Tara Catterall, Christine G Neurauter, Lene Uldal, Rune J Forstrøm and Ann S Langøy (GE Healthcare) for excellent technical assistance. We thank IngenKo, Australia, The Norwegian Transgenic Center (NTS) and the Center for Comparative studies at Rikshospitalet/Radiumhospitalet HF for the excellent service they provided. We also acknowledge the generous financial support provided by the National Program in Functional Genomics (FUGE) sponsored by the Norwegian Research Council, the Norwegian Cancer Society, Throne Holst Foundation and the European Union program 'DNA repair'. We also express our gratitude for the advices and enthusiasm that the late Erling Seeberg provided during the initial phase of the project.

References

Aas PA, Otterlei M, Falnes PO, Vagbo CB, Skorpen F, Akbari M, Sundheim O, Bjoras M, Slupphaug G, Seeberg E, Krokan HE (2003) Human and bacterial oxidative demethylases repair alkylation damage in both RNA and DNA. *Nature* **421:** 859–863

Aravind L, Koonin EV (2001) The DNA-repair protein AlkB, EGL-9, and leprecan define new families of 2-oxoglutarate- and iron-dependent dioxygenases. *Genome Biol* **2**, RESEARCH0007

Barrows LR, Magee PN (1982) Nonenzymatic methylation of DNA by *S*-adenosylmethionine *in vitro*. *Carcinogenesis* **3:** 349–351

Brayton C, Justice M, Montgomery CA (2001) Evaluating mutant mice: anatomic pathology. *Vet Pathol* **38:** 1–19

Chen J, Derfler B, Maskati A, Samson L (1989) Cloning a eukaryotic DNA glycosylase repair gene by the suppression of a DNA repair defect in *Escherichia coli*. *Proc Natl Acad Sci USA* **86:** 7961–7965

Clarke ND, Kvaal M, Seeberg E (1984) Cloning of *Escherichia coli* genes encoding 3-methyladenine DNA glycosylases I and II. *Mol Gen Genet* **197:** 368–372

Crain PF (1990) Preparation and enzymatic hydrolysis of DNA and RNA for mass spectrometry. *Methods Enzymol* **193:** 782–790

Delaney JC, Essigmann JM (2004) Mutagenesis, genotoxicity, and repair of 1-methyladenine, 3-alkylcytosines, 1-methylguanine, and 3-methylthymine in alkB *Escherichia coli*. *Proc Natl Acad Sci USA* **101:** 14051–14056

Delaney JC, Smeester L, Wong C, Frick LE, Taghizadeh K, Wishnok JS, Drennan CL, Samson LD, Essigmann JM (2005) AlkB reverses etheno DNA lesions caused by lipid oxidation *in vitro* and *in vivo*. *Nat Struct Mol Biol* **12:** 855–860

Dinglay S, Trewick SC, Lindahl T, Sedgwick B (2000) Defective processing of methylated single-stranded DNA by *E. coli AlkB* mutants. *Genes Dev* **14:** 2097–2105

Duncan T, Trewick SC, Koivisto P, Bates PA, Lindahl T, Sedgwick B (2002) Reversal of DNA alkylation damage by two human dioxygenases. *Proc Natl Acad Sci USA* **99:** 16660–16665

Engelward BP, Dreslin A, Christensen J, Huszar D, Kurahara C, Samson L (1996) Repair-deficient 3-methyladenine DNA glycosylase homozygous mutant mouse cells have increased sensitivity to alkylation-induced chromosome damage and cell killing. *EMBO J* **15:** 945–952

Engelward BP, Weeda G, Wyatt MD, Broekhof JL, de WJ, Donker I, Allan JM, Gold B, Hoeijmakers JH, Samson LD (1997) Base excision repair deficient mice lacking the Aag alkyladenine DNA glycosylase. *Proc Natl Acad Sci USA* **94:** 13087–13092

Espevik T, Nissen-Meyer J (1986) A highly sensitive cell line, WEHI 164 clone 13, for measuring cytotoxic factor/tumor necrosis factor from human monocytes. *J Immunol Methods* **95:** 99–105

Evensen G, Seeberg E (1982) Adaptation to alkylation resistance involves the induction of a DNA glycosylase. *Nature* **296:** 773–775

Falnes PO (2004) Repair of 3-methylthymine and 1-methylguanine lesions by bacterial and human AlkB proteins. *Nucleic Acids Res* **32:** 6260–6267

Falnes PO, Bjoras M, Aas PA, Sundheim O, Seeberg E (2004) Substrate specificities of bacterial and human AlkB proteins. *Nucleic Acids Res* **32:** 3456–3461

Falnes PO, Johansen RF, Seeberg E (2002) AlkB-mediated oxidative demethylation reverses DNA damage in *Escherichia coli*. *Nature* **419:** 178–182

Falnes PO, Rognes T (2003) DNA repair by bacterial AlkB proteins. *Res Microbiol* **154:** 531–538

Hogan B, Beddington R, Costantini F, Lacy E (1994) *Manipulating the Mouse Embryo; A Laboratory Manual*. Cold Spring Harbor, NY: Cold Spring Harbor Laboratory Press

Karran P, Hjelmgren T, Lindahl T (1982) Induction of a DNA glycosylase for *N*-methylated purines is part of the adaptive response to alkylating agents. *Nature* **296:** 770–773

Karran P, Lindahl T, Griffin B (1979) Adaptive response to alkylating agents involves alteration *in situ* of O6-methylguanine residues in DNA. *Nature* **280:** 76–77

Kataoka H, Sekiguchi M (1985) Molecular cloning and characterization of the alkB gene of *Escherichia coli*. *Mol Gen Genet* **198:** 263–269

Kataoka H, Yamamoto Y, Sekiguchi M (1983) A new gene (alkB) of *Escherichia coli* that controls sensitivity to methyl methane sulfonate. *J Bacteriol* **153:** 1301–1307

Klungland A, Rosewell I, Hollenbach S, Larsen E, Daly G, Epe B, Seeberg E, Lindahl T, Barnes DE (1999) Accumulation of premutagenic DNA lesions in mice defective in removal of oxidative base damage. *Proc Natl Acad Sci USA* **96:** 13300–13305

Koivisto P, Robins P, Lindahl T, Sedgwick B (2004) Demethylation of 3-methylthymine in DNA by bacterial and human DNA dioxygenases. *J Biol Chem* **279:** 40470–40474

Kurowski MA, Bhagwat AS, Papaj G, Bujnicki JM (2003) Phylogenomic identification of five new human homologs of the DNA repair enzyme AlkB. *BMC Genomics* **4:** 48

Laval J (1977) Two enzymes are required from strand incision in repair of alkylated DNA. *Nature* **269:** 829–832

Lee DH, Jin SG, Cai S, Chen Y, Pfeifer GP, O'connor TR (2005) Repair of methylation damage in DNA and RNA by mammalian AlkB homologues. *J Biol Chem* **280:** 39448–39458

Lindahl T (1993) Instability and decay of the primary structure of DNA. *Nature* **362:** 709–715

Mackay WJ, Han S, Samson LD (1994) DNA alkylation repair limits spontaneous base substitution mutations in *Escherichia coli*. *J Bacteriol* **176:** 3224–3230

Mukherji M, Chien W, Kershaw NJ, Clifton IJ, Schofield CJ, Wierzbicki AS, Lloyd MD (2001) Structure-function analysis of phytanoyl-CoA 2-hydroxylase mutations causing Refsum's disease. *Hum Mol Genet* **10:** 1971–1982

Naslund M, Segerback D, Kolman A (1983) *S*-adenosylmethionine, an endogenous alkylating agent. *Mutat Res* **119:** 229–232

Ougland R, Zhang CM, Liiv A, Johansen RF, Seeberg E, Hou YM, Remme J, Falnes PO (2004) AlkB restores the biological function of mRNA and tRNA inactivated by chemical methylation. *Mol Cell* **16:** 107–116

Relyea MJ, Miller J, Boggess D, Sundberg J (2000) Necropsy methods for laboratory mice: biological characterization of a new mutation. In *Systematic Approach to Evaluation of Mouse Mutations*, Sundberg P, Boggess D (eds), pp 57–89. Boca Raton: CRC Press

Rozenski J, Crain PF, McCloskey JA (1999) The RNA Modification Database: 1999 update. *Nucleic Acids Res* **27:** 196–197

Rydberg B, Lindahl T (1982) Nonenzymatic methylation of DNA by the intracellular methyl group donor *S*-adenosyl-L-methionine is a potentially mutagenic reaction. *EMBO J* **1:** 211–216

Saintigny Y, Delacote F, Vares G, Petitot F, Lambert S, Averbeck D, Lopez BS (2001) Characterization of homologous recombination induced by replication inhibition in mammalian cells. *EMBO J* **20:** 3861–3870

Sedgwick B (2004) Repairing DNA-methylation damage. *Nat Rev Mol Cell Biol* **5:** 148–157

Tano K, Shiota S, Collier J, Foote RS, Mitra S (1990) Isolation and structural characterization of a cDNA clone encoding the human DNA repair protein for O6-alkylguanine. *Proc Natl Acad Sci USA* **87:** 686–690

Taverna P, Sedgwick B (1996) Generation of an endogenous DNA-methylating agent by nitrosation in *Escherichia coli*. *J Bacteriol* **178:** 5105–5111

Trewick SC, Henshaw TF, Hausinger RP, Lindahl T, Sedgwick B (2002) Oxidative demethylation by *Escherichia coli* AlkB directly reverts DNA base damage. *Nature* **419:** 174–178

Valegard K, Terwisscha van Scheltinga AC, Dubus A, Ranghino G, Oster LM, Hajdu J, Andersson I (2004) The structural basis of cephalosporin formation in a mononuclear ferrous enzyme. *Nat Struct Mol Biol* **11:** 95–101

Wei YF, Carter KC, Wang RP, Shell BK (1996) Molecular cloning and functional analysis of a human cDNA encoding an *Escherichia coli* AlkB homolog, a protein involved in DNA alkylation damage repair. *Nucleic Acids Res* **24:** 931–937

Wu RS, Hurst-Calderone S, Kohn KW (1987) Measurement of O6-alkylguanine-DNA alkyltransferase activity in human cells and tumor tissues by restriction endonuclease inhibition. *Cancer Res* **47:** 6229–6235

Yu B, Edstrom WC, Benach J, Hamuro Y, Weber PC, Gibney BR, Hunt JF (2006) Crystal structures of catalytic complexes of the oxidative DNA/RNA repair enzyme AlkB. *Nature* **439:** 879–884

